

Learning to Compress and Transmit: Adaptive Rate Control for Semantic Communications over LEO Satellite-to-Ground Links

Jiangtao Luo, *Senior Member, IEEE*, Yongyi Ran, *Member, IEEE*, Guoliang Xu and Jihua Zhou

Abstract—The bottleneck of satellite-to-ground links poses a major challenge for the timely downlink of massive on-board imagery. This paper studies adaptive image transmission over LEO satellite-to-ground links using joint source-channel coding (JSCC). We propose an RL-based framework that dynamically selects the channel dimension (compression ratio) of a Swin-JSCC encoder to maximize the number of receivedes satisfying reconstruction-quality constraints (PSNR and MS-SSIM) within a finite visibility window. The agent leverages SNR prediction to perform proactive rate adaptation and incorporates an on-board transmission-queue model that captures bursty encoding while penalizing both buffer overflow and underutilization. Simulations under realistic overpass conditions show that the proposed policy substantially outperforms fixed-rate baselines, achieving nearly 95% qualified frames with zero packet loss.

Index Terms—semantic communications, joint source channel coding, low-Earth-orbit satellites, satellite-to-ground links, deep reinforcement learning.

I. INTRODUCTION

THE rapid growth of data generated aboard low Earth orbit (LEO) satellites poses a critical challenge: how to efficiently transmit this data back to the ground. Traditional pixel-wise compression methods, such as JPEG2000, BPG, and emerging deep learning-based approaches including DeepSpace [1], have approached their fundamental limits yet still struggle to meet the increasing demands of high-throughput satellite missions. On the other hand, on-board artificial intelligence (AI) processing offers an alternative, but remains severely constrained by the extremely limited computational and energy resources available on satellite platforms.

Semantic communication [2] has emerged as a promising paradigm to address this challenge. Instead of transmitting raw pixels, a semantic encoder extracts and transmits compact semantic features to the ground, where a decoder reconstructs the original image. This approach offers two key advantages. First, it significantly reduces the amount of data to be transmitted, alleviating the bottleneck of limited downlink bandwidth. Second, semantic communication exhibits inherent robustness to channel variations, effectively overcoming the well-known “cliff effect” that plagues conventional digital communication systems. This makes it particularly suitable for dynamic LEO satellite-to-ground links, where channel conditions vary rapidly over time.

Jiangtao Luo, Yongyi Ran and Guoliang Xu are with the School of Communications and Information Engineering, Chongqing University of Posts and Telecommunications, Chongqing, 400065 China. Jihua Zhou is with the College Of Computer and Information Science, Southwest University, Chongqing 400715, China. Jiangtao Luo and Yongyi Ran are the corresponding authors. (Email: Luoijt@cqupt.edu.cn, ranyy@cqupt.edu.cn).

This work is supported by the National Natural Science Foundation of China (No. U25B2033, No. 62171072 and No. U23A20275).

A prominent implementation of semantic communication is deep joint source-channel coding (DeepJSCC) [3], which integrates source coding, channel coding, and modulation into a single end-to-end optimized neural network. Unlike traditional separation-based schemes that optimize source and channel modules independently, DeepJSCC learns a joint representation that is directly mapped to channel input symbols. This approach not only eliminates the cliff effect by gracefully degrading reconstruction quality as channel conditions worsen, but also achieves superior performance at low signal-to-noise ratios (SNR) and limited bandwidth regimes. Building upon this foundation, [4] proposed SwinJSCC, which replaces the convolutional neural network (CNN) backbone with a Swin Transformer architecture. The SwinJSCC encoder leverages hierarchical feature extraction and window-based self-attention mechanisms to capture long-range dependencies in images, leading to improved reconstruction quality, especially for high-resolution imagery. Furthermore, SwinJSCC incorporates two plug-in modules – *Channel ModNet* and *Rate ModNet* – that enable a single model to adapt flexibly to varying channel SNR and transmission rates, making it particularly attractive for dynamic satellite communication scenarios.

Despite its potential, research on semantic communication for satellite links, especially for LEO feeder links, remains limited. Several critical aspects unique to satellite communications have been largely overlooked in existing work. First, most semantic communication frameworks assume an idealized setting where the encoder has instantaneous and perfect knowledge of the channel state, and where the transmission itself incurs negligible delay. In practice, however, LEO satellite links exhibit non-negligible propagation delays that vary with the elevation angle, typically ranging from several to tens of milliseconds. These delays, combined with the uplink command transmission and on-board processing, introduce a control loop latency that can render decisions based on current channel observations outdated by the time the corresponding signal is actually transmitted. Second, existing studies rarely consider the impact of on-board transmission buffering. In a satellite system, encoded symbols must be queued before transmission, and the queue dynamics – influenced by both the selected compression ratio and the time-varying channel symbol rate – directly affect the system’s ability to avoid buffer overflow and maximize throughput. To the best of our knowledge, no prior work on semantic communication has systematically addressed the coupled challenges of propagation-induced control latency and queue-aware rate adaptation for LEO satellite links.

In this paper, we target the efficient downlink transmission of observed images from LEO satellites to ground gateways.

We propose an adaptive semantic communication framework based on SwinJSCC, a joint source-channel coding scheme built upon the Swin Transformer architecture. The objective is to maximize the number of successfully transmitted images that meet predefined quality requirements (in terms of PSNR and MS-SSIM) within a single satellite overpass. To cope with the time-varying channel conditions and control loop latency, we further integrate a reinforcement learning agent with SNR prediction to dynamically adjust the compression ratio of the SwinJSCC encoder. The proposed framework operates in a *predict–decide–execute* paradigm, where the ground gateway forecasts future channel states, selects an optimal compression ratio, and sends the decision to the satellite for execution. Extensive simulations demonstrate that our approach significantly outperforms fixed-rate and threshold-based strategies in terms of both throughput and image quality.

The main contributions of this paper are summarized as follows:

- **Queue-aware and latency-resilient rate control:** We identify two critical but overlooked challenges in semantic communication for LEO satellites: elevation-dependent propagation delays that induce control loop latency, and on-board transmission queue dynamics that affect throughput. To address these, we introduce a *predict–decide–execute* framework that integrates SNR predictors for future SNR leveraging link budget, enabling the RL agent to select compression ratios aligned with future channel and buffer states.
- **Ground-based deployment with closed-loop telemetry:** We propose a practical deployment architecture where the RL agent and SNR predictor reside at the ground gateway. The satellite periodically downlinks queue length telemetry, while the gateway estimates SNR from received signals. Uplink commands deliver both the selected compression ratio and the predicted SNR to the satellite, where the Channel ModNet and Rate ModNet update accordingly.
- **Comprehensive simulation and performance evaluation:** We build a realistic LEO feeder link simulator incorporating elevation-dependent SNR trajectories and variable propagation delays. Extensive overpass-level simulations demonstrate that our approach increases the number of successfully transmitted images by up to 5% compared to fixed-rate baselines strategies, while maintaining stable queue occupancy and meeting quality constraints.

II. RELATED WORK

A. Joint Source-Channel Coding for Image Transmission

Deep joint source-channel coding (DeepJSCC) has emerged as a promising paradigm for wireless image transmission, eliminating the “cliff effect” inherent in separate source and channel coding. [3] established the theoretical foundation for semantic communication networks, paving the way for practical DeepJSCC implementations. Building on this foundation, [5] proposed ADJSCC which introduced attention modules into DeepJSCC, enabling the model to adaptively

focus on informative features and significantly improving its performance, particularly at low signal-to-noise ratios (SNR) where it outperforms conventional separation-based schemes. Subsequently, [4] proposed SwinJSCC, which replaces the CNN backbone with a Swin Transformer, achieving superior performance for high-resolution images through hierarchical feature extraction and window-based self-attention. SwinJSCC also introduces Channel ModNet and Rate ModNet modules, enabling a single model to adapt to varying channel conditions and transmission rates.

B. Related Work on Adaptive Deep JSCC for Satellite Communications

Existing adaptive deep joint source-channel coding (JSCC) methods for satellite image transmission can be broadly categorized into two families based on their backbone architecture: convolutional neural network (CNN) based and Vision Transformer (ViT) based. Each family shares common limitations that are particularly critical for LEO satellite links.

a) CNN-based Approaches.: Several works adopt CNN-based DeepJSCC as their foundation. [6] formulates a resource allocation problem for DeepJSCC-based satellite transmission, jointly optimizing image resolution, information entropy, latency, and power via linear programming. [7] proposes ASE-JSCC, which jointly optimizes remote sensing image transmission with downstream classification tasks, achieving high compression ratios (up to $384\times$) through semantic feature selection and noise-injected training. Most recently, [8] presents ARJSCC, which adapts semantic feature extraction to varying SNR via an attention module, adjusts semantic length via a position mask, and transmits a compressed residual with a dedicated enhancement model.

Despite their innovations, all CNN-based approaches share a fundamental limitation: the inherently limited receptive field and model capacity of CNNs, which struggle to capture long-range dependencies in high-resolution remote sensing images. Moreover, they commonly assume instantaneous channel feedback and negligible transmission delay, overlooking the elevation-dependent propagation delays and the timeliness requirements of real-time data delivery. On-board queue dynamics, which directly affect throughput and delay in satellite systems, are also ignored. Consequently, these methods are ill-suited for dynamic LEO satellite links where control latency and buffer management are critical.

b) ViT-based Approaches.: To overcome the capacity constraints of CNNs, some works turn to Vision Transformers. [9] proposes SatSemCom, which features a ViT-based semantic encoder, a channel predictor to mitigate outdated CSI, and a rate adaptation module. [10] introduces a ViT-based JSCC approach for multi-modal satellite-to-ground communication, learning common semantic information across modalities to reduce coding space.

However, ViT-based encoders suffer from quadratic computational complexity with respect to image resolution, limiting their scalability to high-resolution imagery (e.g., the reported input size in [10] is only $3\times 512\times 512$). In contrast, hierarchical architectures like Swin Transformer achieve linear complexity

via shifted window attention. Furthermore, like their CNN counterparts, these ViT-based methods also neglect on-board queue dynamics and elevation-dependent propagation delays, which are essential for real-time adaptive transmission over LEO links.

c) Predictive and Adaptive Coding.: [11] proposes PADC, a predictive framework that minimizes transmission rate under PSNR constraints by predicting reconstruction quality from image content, SNR, and compression ratio. While effective in general settings, its transmitter-side prediction module imposes on-board computation that is challenging for resource-constrained LEO satellites. It also assumes instantaneous feedback and does not address control latency or queue dynamics.

In summary, existing CNN-based JSCC methods lack the capacity to handle high-resolution imagery, while ViT-based methods face quadratic complexity. Nearly all assume instantaneous feedback and ignore propagation-induced latency, on-board queue dynamics, and adaptive rate control over a complete satellite overpass. These gaps motivate our work, which combines a Swin Transformer-based JSCC encoder (offering linear complexity) with a ground-based RL agent, link-budget based SNR prediction, and a queue-aware reward design tailored for LEO satellite links.

C. Positioning of This Work

In contrast to the above, existing semantic and joint source-channel coding methods for satellite image transmission suffer from several common limitations: limited model capacity (CNN-based), quadratic complexity (ViT-based), neglect of propagation delays and on-board queue dynamics, transmitter-side predictive burden, and lack of joint optimization over a full overpass.

This paper advances the state of the art by (i) adopting SwinJSCC with linear complexity for high-resolution multispectral images, (ii) explicitly addressing control loop latency via SNR prediction in a predict–decide–execute paradigm, (iii) incorporating queue dynamics into RL state and reward for proactive congestion control, (iv) deploying the RL agent and predictor on the ground to minimize on-board computation, and (v) optimizing over a complete satellite overpass to maximize qualified frames under quality constraints. Simulations demonstrate significant gains over fixed-rate baselines.

III. SYSTEM MODEL AND PROBLEM FORMULATION

A. System Model

The system model is illustrated in Fig. 1. We consider a low Earth orbit (LEO) Earth observation satellite transmitting captured images to a ground gateway. To cope with the dynamic loss characteristics of the satellite-to-ground link (GSL), a semantic encoder (SemEncoder) based on the SwinJSCC scheme is deployed on board. Specifically, each original image is first semantically encoded by the SemEncoder, and the resulting symbols are placed into a transmission queue before being sent over the GSL. Upon reception, the ground gateway reconstructs the image using the corresponding semantic decoder (SemDecoder).

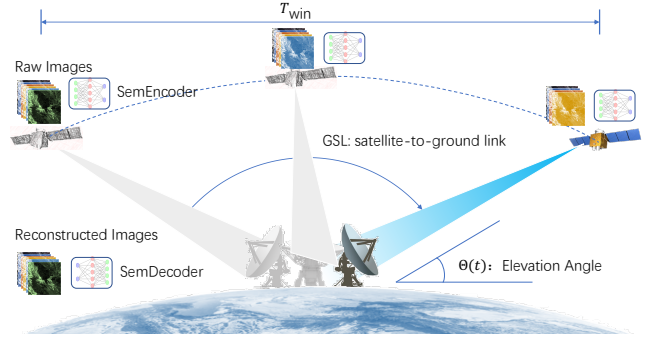


Fig. 1. System architecture of semantic communications for multispectral images over GSL.

The GSL considered in this work is the feeder link from the satellite to the ground gateway. We adopt the additive white Gaussian noise (AWGN) channel as the baseline model, augmented with a constant additional attenuation margin (e.g., 2.5 dB) to account for simplified atmospheric effects, rather than explicitly modeling rain fading or tropospheric scintillation. More realistic random or bursty impairments can be incorporated in future extensions. The variation of SNR with satellite elevation angle over a single overpass is explicitly characterized. Unlike the original SwinJSCC studies that assume an idealized channel with stationary statistics, our work introduces two key practical considerations: an on-board transmission queue to model buffer dynamics, and the time-varying SNR trajectory over the satellite visibility window, which captures the realistic evolution of link quality during an overpass.

B. Channel Model for LEO Feeder Link

The LEO satellite-to-gateway (feeder) downlink is modeled as an additive white Gaussian noise (AWGN) channel with time-varying signal-to-noise ratio (SNR). The received power $P_r(t)$ varies deterministically with the satellite elevation angle $\theta(t)$ over a visibility window of approximately 600 seconds (assuming a 900 km orbit altitude), following:

$$P_r(t) = \underbrace{(P_t + G_t)}_{\text{EIRP}} + G_r - L, \quad (\text{dB}),$$

where P_t is the satellite transmit power (dBW), G_t and G_r are the antenna gains of the satellite and the ground gateway (dBi), respectively, and $L = L_{\text{FSPL}}(t) + L_{\text{extra}}(t)$ denotes the total loss (dB), which includes the free-space path loss $L_{\text{FSPL}}(t)$ and all additional atmospheric losses $L_{\text{extra}}(t)$ (such as gas absorption, rain attenuation, and other impairments). The instantaneous SNR, denoted as $\gamma(t)$, is given by $\gamma(t) = P_r(t) - N_0 - 10 \log_{10}(B_n)$, where N_0 is the noise power spectral density (in dBW/Hz or dBm/Hz), and B_n is the receiver noise bandwidth (in Hz).

The AWGN simplification is justified by the gateway's high-gain directional antenna and open-area deployment, which effectively eliminate multipath propagation. In an AWGN channel, the multiplicative distortion is a purely amplitude-scaling factor $\sqrt{P_r(t)}$, which is *deterministic and known* from

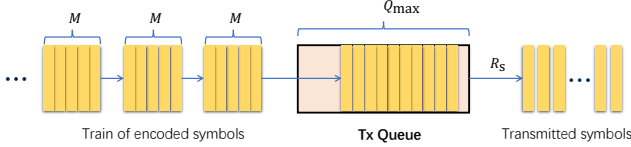


Fig. 2. Transmit queue model.

the satellite's trajectory. This is fundamentally different from a fading channel, where the amplitude scaling is a *random, unknown* process. The received complex baseband signal is therefore expressed as:

$$y(t) = \sqrt{P_r(t)} \cdot x(t) + n(t), \quad n(t) \sim \mathcal{CN}(0, N_0).$$

In engineering practice, the link performance of the satellite-to-ground feeder link is preferred to be compactly expressed using the satellite effective isotropic radiated power (EIRP), the ground station figure of merit G/T , and the carrier-to-noise density ratio C/N_0 . The fundamental link equation for C/N_0 is given by:

$$C/N_0 = \text{EIRP} - L + G/T - 10 \log_{10}(k) \quad (\text{dBHz}), \quad (1)$$

where $k = 1.380649 \times 10^{-23}$ J/K is Boltzmann's constant, and $10 \log_{10}(k) \approx -228.6$ dBW/K/Hz. The instantaneous signal-to-noise ratio $\gamma(t)$ is then obtained from C/N_0 by accounting for the receiver noise bandwidth B_n :

$$\gamma(t) = C/N_0 - 10 \log_{10}(B_n) \quad (\text{dB}). \quad (2)$$

In this paper, this formulation directly links the engineering parameters (EIRP, G/T) to the SNR used in our channel model, providing a practical and modular approach for link budget calculations and ensuring alignment with realistic engineering parameters.

C. Symbol-Level Transmit Queue Model

To bridge the gap between the bursty output of the semantic encoder and the constant-rate physical layer, we introduce a transmission queue for encoded symbols at the satellite. This queue absorbs short-term fluctuations in symbol generation and provides a realistic abstraction of on-board buffering constraints.

1) *Queue Dynamics*: To improve computational efficiency and fully exploit the parallel processing capabilities of neural network accelerators (e.g., GPUs or on-board NPUs), we adopt a batch-wise encoding strategy that naturally matches the bursty nature of semantic encoding. Processing a batch of images in a single forward pass significantly reduces the number of kernel launches and memory transfers compared to sequential single-image processing, thereby lowering inference latency and on-board energy consumption. Let T_d denote the decision interval, which defines the period over which the agent selects a compression ratio. Within each decision interval, the encoder processes a batch of M images, as illustrated in Fig. 2. For a given compression ratio R_t , the number of symbols generated for a single image is $N_{\text{sym}}(R_t)$; consequently, a batch of M images produces a total of

$A_t = M \times N_{\text{sym}}(R_t)$ symbols. After encoding, these symbols are pushed into the transmission queue sequentially, one image at a time.

The physical layer transmits symbols at a constant rate R_s (symbols per second), which is determined by the signal bandwidth B_s and the pulse shaping filter. Specifically, for a system with bandwidth B_s and a raised-cosine filter with roll-off factor α , the symbol rate is given by $R_s = B_s/(1 + \alpha)$. Under ideal low-pass filtering ($\alpha \rightarrow 0$) and no channel distortions, we have the approximation $R_s \approx B_s$.

Let Q_t denote the queue length (in symbols) at the beginning of time slot t . The queue evolves as symbols are added from encoded images and removed by the physical layer at rate R_s . The number of symbols that can be transmitted during one decision interval of length T_d is $R_s T_d$. Thus, the queue update is given by:

$$Q_{t+1} = \max(0, Q_t + A_t - R_s \cdot T_d),$$

where $\max(\cdot)$ ensures that the queue length never becomes negative (idle periods are allowed), and A_t is the total number of symbols generated in time slot t .

2) *Two Queue Indicators*: The queue update equation Q_{t+1} presented earlier (assuming an infinite buffer) provides an idealized evolution assuming an infinite buffer. In practice, the satellite has finite on-board memory, which imposes a hard upper bound on the queue length. This maximum queue capacity, denoted Q_{max} , must be explicitly defined to capture buffer overflow and the resulting image discards.

We introduce two indicators to characterize the transmission queue behavior:

- **Queue Capacity Indicator (QCI)**, q_c : The maximum queue length Q_{max} is set to accommodate the maximum symbol arrival over q_c consecutive decision intervals under the highest compression ratio:

$$Q_{\text{max}} = q_c \times M \times N_{\text{sym}}^{\text{max}},$$

where $N_{\text{sym}}^{\text{max}}$ is the number of symbols per image when the maximum allowed compression ratio (or channel number) is selected. The parameter q_c controls the buffer depth in units of decision intervals, balancing robustness against bursty arrivals against on-board memory constraints.

- **Queue Drain Indicator (QDI)**, q_d : This indicator represents the number of decision intervals required to completely empty a full queue. The drain rate is determined by the physical layer symbol rate R_s and the decision interval length T_d , hence:

$$q_d = \left\lceil \frac{Q_{\text{max}}}{R_s T_d} \right\rceil.$$

q_d reflects the time needed to recover from a worst-case buffer occupancy and measures the system's responsiveness under congestion.

Specifically, using the Kodak image dimensions (768×512 pixels, RGB) and a maximum channel number $C_K = 192$, we compute $N_{\text{sym}}^{\text{max}} = 147,456$ symbols per image. With $q_c = 3$ and $M = 15$, the queue capacity is $Q_{\text{max}} = 6,635,520$ symbols. Setting $q_d = 6$ yields a per-decision-interval transmission

budget of $S_{\text{tx}} = R_s \cdot T_d \approx 1.11 \times 10^6$ symbols. For a decision interval $T_d = 5$ s, the required physical layer symbol rate is $R_s \approx 0.22$ Msym/s; for $T_d = 1$ s, $R_s \approx 1.11$ Msym/s. These values confirm the feasibility of the proposed queue model under realistic LEO satellite link budgets.

3) *Discard Policy*: When pushing the M encoded images of a batch into the queue, we check the available space before adding each image. For the j -th image in the batch ($j = 1, \dots, M$), if the current queue length Q satisfies $Q + N_{\text{sym}}(R_t) \leq Q_{\text{max}}$, the image is successfully queued. Otherwise, the image is discarded, and no further images from the same batch are queued (i.e., discarding is sequential and stops at the first failure). Consequently, a batch may result in d discarded images, where $0 \leq d \leq M$, and only $M - d$ images are successfully transmitted in that decision interval. This per-image discard policy preserves the semantic integrity of each transmitted image — an image is either fully queued or completely discarded — while allowing partial batch transmission to maximize throughput under congestion.

To discourage discards, the RL agent receives a penalty proportional to the number of discarded images d in each decision interval. This incentivizes the agent to proactively reduce the compression ratio R_t when the queue length approaches Q_{max} , thereby avoiding buffer overflow and ensuring reliable transmission.

For long-term stability, the average arrival rate must not exceed the average service rate:

$$\frac{1}{2}M \times P \times \mathbb{E}[R_t] < R_s \times T_d,$$

where $\mathbb{E}[R_t]$ is the expected compression ratio under the learned policy. This condition is naturally enforced by the RL reward design, which penalizes queue buildup and discards.

The queue serves three critical functions in our framework. First, it decouples the semantic encoder (which operates in bursts) from the physical layer (which transmits continuously), allowing each to operate at its own pace. Second, the queue length Q_t provides a direct measure of congestion, which is fed back to the RL agent via the telemetry downlink. By observing Q_t , the agent learns to reduce the compression ratio R_t when the queue builds up, and to increase it when the queue is empty, thereby balancing transmission efficiency and buffer occupancy. Third, the per-image discard policy preserves semantic integrity, while the associated penalty guides the agent toward congestion-aware rate adaptation.

D. Problem Formulation

We consider a LEO satellite downlink communications system where a satellite transmits a sequence of images to a ground gateway during a single visibility window of duration T_{win} seconds. The satellite is equipped with a SwinJSCC encoder that compresses each image into a variable-length complex symbol vector based on a compression ratio $R \in \mathcal{R}$, where $\mathcal{R} = \{R_1, R_2, \dots, R_K\}$ is a discrete set of admissible ratios.

The communication channel is time-varying due to satellite motion, atmospheric effects (rain fading, scintillation), and potential interference. At each time step t , the channel quality

is characterized by the signal-to-noise ratio $\text{SNR}(t)$, which depends on the satellite elevation angle $\theta(t)$ and stochastic environmental conditions.

1) *System Dynamics*: Let $\mathcal{T} = \{1, 2, \dots, T\}$ denote the set of decision epochs, where T is the total number of decision steps within the visibility window (e.g., each step corresponds to one second). At each epoch t , the system is described by the following state vector:

$$\mathbf{s}_t = (\gamma_t, \theta_t, Q_t, R_{t-1}) \in \mathcal{S}, \quad (3)$$

where $\gamma_t \in \mathbb{R}^+$ is the estimated SNR at time step t ; $\theta_t \in [\theta_{\min}, 90^\circ]$ is the satellite elevation angle; $Q_t \in [0, Q_{\text{max}}]$ is the current length of the transmission buffer (in symbols); $R_{t-1} \in \mathcal{R}$ is the compression ratio selected at the previous decision epoch.

2) *Action Space*: The agent selects a discrete action at each decision epoch. Let $\mathcal{R} = \{R_1, R_2, \dots, R_K\}$ denote the finite set of admissible compression ratios, where K is the number of discrete choices. For each $k \in \{1, \dots, K\}$, $R_k \in (0, 1]$ represents a specific compression ratio supported by the SwinJSCC encoder.

At decision epoch t , the agent selects an action $a_t = R_t \in \mathcal{R}$, where R_t is the target bandwidth ratio (compression ratio) to be applied to the next image. The action space is therefore $\mathcal{A} = \mathcal{R}$, with cardinality $|\mathcal{A}| = K$.

When action $a_t = R_k$ is selected, the number of complex symbols generated by the SwinJSCC encoder for the next image is determined by the bandwidth ratio R_k and the total number of pixels in the original image. Let $P_{\text{in}} = H \times W \times C_{\text{in}}$ denote the total number of input pixels per image, where $C_{\text{in}} = 3$ for RGB images. The number of transmitted symbols per encoded image is then given by:

$$N_{\text{sym}}(R_t) = \frac{P_{\text{in}}}{2} \times R_t = \frac{1}{2} \times \frac{H}{2^i} \times \frac{W}{2^i} \times C_t = S_{\text{iHW}} \times C_t, \quad (4)$$

where i is the number of stages in the SwinJSCC encoder, and $C_t \in \mathcal{C} = \{C_1, C_2, \dots, C_K\}$ denotes the number of channels selected by the agent for the Rate ModNet at decision step t , i.e., C_t corresponds to the compression ratio R_t . Here, $S_{\text{iHW}} = \frac{1}{2} \times \frac{H}{2^i} \times \frac{W}{2^i}$ is a constant determined by the input image dimensions and the number of stages in the SwinJSCC encoder. Specifically, following the 4-stage SwinJSCC encoder [4], there are five levels of channel numbers, i.e., $\mathcal{C} = \{32, 64, 96, 128, 192\}$, which correspond to the compression ratio set $\mathcal{R} = \{1/48, 1/24, 1/16, 1/12, 1/8\}$. This formulation directly follows the definition of the bandwidth ratio in the original SwinJSCC work, where R_t represents the ratio between the number of transmitted symbols and the number of input pixels. The generated symbols are then appended to the transmission buffer and wait for transmission.

3) *Reward Function*: An image is considered successfully transmitted if its reconstruction quality meets predefined thresholds Γ_{PSNR} and $\Gamma_{\text{MS-SSIM}}$. The immediate reward is defined as:

$$r_t = \begin{cases} 1, & \text{if } \text{PSNR}_t \geq \Gamma_{\text{PSNR}} \text{ and } \text{MS-SSIM}_t \geq \Gamma_{\text{MS-SSIM}}, \\ 0, & \text{otherwise.} \end{cases} \quad (5)$$

To enforce system constraints and encourage efficient buffer utilization, we augment the reward with two queue-related penalty terms.

First, when the queue length exceeds the threshold Q_{th} , we apply a linear penalty that grows with the degree of overflow:

$$p_{\text{over}}(t) = \lambda_{\text{over}} \cdot \max\left(0, \frac{Q_t - Q_{\text{th}}}{Q_{\text{max}} - Q_{\text{th}}}\right),$$

where λ_{over} is a coefficient controlling the severity of the penalty, and the fraction normalizes the excess to $[0, 1]$. This term discourages the agent from allowing the queue to approach saturation.

Second, to prevent the queue from staying unnecessarily empty (which may indicate underutilization of the downlink), we introduce a small penalty when the normalized queue length is below a lower threshold Q_{low} :

$$p_{\text{under}}(t) = \lambda_{\text{under}} \cdot \mathbf{1}_{\{Q_t \leq Q_{\text{low}}\}},$$

where λ_{under} is a small positive coefficient. This term gently encourages the agent to maintain a minimal buffer occupancy, avoiding excessive idle periods.

Additionally, a discard penalty remains for images dropped due to queue overflow:

$$p_{\text{drop}}(t) = \lambda_d \cdot d_t,$$

where d_t is the number of discarded images in time slot t .

The overall augmented reward is then:

$$\tilde{r}_t = r_t - p_{\text{over}}(t) - p_{\text{under}}(t) - p_{\text{drop}}(t),$$

where $r_t = \mathbf{1}_{\{\text{PSNR}_t \geq \Gamma_{\text{PSNR}} \wedge \text{MS-SSIM}_t \geq \Gamma_{\text{MS-SSIM}}\}}$ is the success indicator for transmitted images (defined in Eq. (5)).

4) *Optimization Objective*: We formulate the problem as a finite-horizon, discrete-time Markov decision process (MDP) defined by the tuple $(\mathcal{S}, \mathcal{A}, P, \tilde{r}, T)$, where \mathcal{S} is the state space; \mathcal{A} is the action space; P is the transition probability, defined implicitly by the system dynamics (i.e., the evolution of SNR, elevation angle and buffer length); \tilde{r} is the reward function, and T is the horizon. The goal is to find an optimal policy π^* that maximizes the expected cumulative reward, which corresponds to transmitting as many qualified images as possible within each visibility window:

$$\pi^* = \arg \max_{\pi} \mathbb{E}_{\pi} \left[\sum_{t=1}^T \tilde{r}_t \right], \quad (6)$$

subject to:

$$\text{PSNR}_t \geq \Gamma_{\text{PSNR}}, \quad \forall t, \quad (7)$$

$$\text{MS-SSIM}_t \geq \Gamma_{\text{MS-SSIM}}, \quad \forall t, \quad (8)$$

$$Q_t \leq Q_{\text{max}}, \quad \forall t, \quad (9)$$

$$\sum_{t=1}^T T_{\text{tx}}(R_t) \leq T_{\text{win}}. \quad (10)$$

IV. PROPOSED APPROACH

The overall architecture of our proposed GSL-SwinJSCC is illustrated in Fig. 3. The images captured by the satellite are first processed by a SwinJSCC encoder, which extracts semantic features. The encoder is fine-tuned to accommodate the GSL SNR range (1–38 dB), ensuring robust performance across the full overpass. After channel and rate modulation, the encoded features are placed into a transmission queue. The queue is introduced to accommodate the limited on-board storage capacity and the bandwidth bottleneck of GSL. The transmission queue has a maximum symbol capacity of Q_{max} and transmits the features to the ground receiver at a constant symbol rate R_s over the GSL data channel. At the ground side, the received signals undergo feature reconstruction and image restoration, leveraging both the SNR estimated by an SNR detector and the mask vector used for rate modulation, which is received via the control channel.

To fully utilize the downlink bandwidth and cope with the long delay and dynamic nature of the GSL, we introduce a DRL agent along with an SNR predictor. The predictor forecasts the future SNR based on GSL link budget. The predicted SNR serves as the input to the on-board channel modulation module, and together with the current queue length and the ground elevation angle, forms the system state variables. Based on this state, the DRL agent determines an optimized compression ratio R , which serves as the target rate for the rate modulation network. These control parameters are reliably transmitted via the satellite's tracking, telemetry, and command (TT&C) system.

A. Prediction-Aligned Control

Although the LEO feeder link is well approximated by an AWGN model with deterministic SNR variations, the physical propagation delay and the uplink command transmission introduce a non-negligible control loop latency of approximately 10–15 ms. During this interval, the satellite elevation angle and consequently the SNR γ_t can change significantly, especially at low elevation angles where the SNR slope is steep. Moreover, the satellite's transmission buffer occupancy Q_t evolves dynamically in response to previous compression decisions and the constant symbol rate of the physical layer. A decision made based on the current SNR γ_t and buffer length Q_t may therefore become outdated by the time the corresponding image is actually transmitted, leading to suboptimal compression ratio selection, buffer overflow, or quality degradation.

To address this mismatch, the reinforcement learning agent is deployed at the ground gateway to leverage its abundant computational resources. The architecture follows a *predict–decide–execute* paradigm that compensates for the inherent control loop latency in LEO satellite links.

1) *Downlink Telemetry and Prediction*: The satellite periodically samples its transmission buffer occupancy Q_t and encapsulates this information into CCSDS-compliant telemetry frames transmitted to the ground gateway. Concurrently, the ground gateway estimates the downlink SNR γ_t from the received signal using embedded pilots or preamble sequences.

decreases back to 20° over a complete visibility window, the corresponding SNR varies between approximately 26 dB and 34 dB. The decision interval is set to $T_d = 5$ seconds, and the encoder processes $M = 12$ images per decision interval. Each image has a resolution of 768×512 pixels (Kodak24) with $C_{in} = 3$ channels (RGB). The SwinJSCC model used in all experiments is the fine-tuned version described in Section V, which supports SNR ranging from 1 dB to 38 dB. The quality thresholds are set to $\Gamma_{PSNR} = 32$ dB and $\Gamma_{MS-SSIM} = 0.94$ by default.

2) *Compared Algorithms*: We compare our proposed method against the following baseline policies:

- **Fixed Maximum Rate** (`max_rate`): The encoder always uses the maximum allowed number of channels ($C = 192$) to transmit semantic features for every image.
- **Fixed Medium Rate** (`mid_rate`): The encoder always uses the medium allowed number of channels ($C = 96$) for every image.
- **Fixed Minimum Rate** (`min_rate`): The encoder always uses the minimum allowed number of channels ($C = 32$) for every image.
- **DQN** (`rl_dqn`): A standard Deep Q-Network for rate adaptation.

3) *Evaluation Metrics*: We adopt the following metrics to evaluate the performance of different rate adaptation policies.

- **Qualified Frames** (Q_{qual}): The number of successfully transmitted images that meet both quality thresholds, i.e., $PSNR \geq \Gamma_{PSNR}$ and $MS-SSIM \geq \Gamma_{MS-SSIM}$, accumulated over a complete satellite overpass. This is the primary measure of effective throughput.
- **Forwarding Efficiency** (η_1): Defined as $\eta_1 = Q_{qual}/F$, where F denotes the number of frames that leave the transmission queue and are transmitted over the wireless channel (i.e., forwarded frames). This metric captures the proportion of transmitted frames that ultimately become qualified. It penalizes policies that waste on-board computational resources, storage, and transmission power on frames that fail to meet the quality requirements.

B. Training

1) *Fine-tune of SwinJSCC*: The pre-trained SwinJSCC model is trained on AWGN channels with SNR values ranging from 1 to 13 dB. However, our link-budget based GSL SNR sequence exhibits a wider dynamic range: the SNR reaches approximately 34 dB at zenith under clear-sky conditions, significantly exceeding the upper bound of the original pre-trained model.

To address this domain gap, we fine-tune the pre-trained SwinJSCC model on our GSL-specific SNR distribution. Specifically, we adopt the versatile version equipped with both Channel Adaptation (SA) and Rate Adaptation (RA) modules. The pre-trained weights of the Swin Transformer backbone are preserved as initialization, while the model is further trained on simulated channel conditions covering the full SNR range observed in our GSL scenarios. Notably, the primary focus of fine-tuning is on the SNR values corresponding to elevation angles above 20° , which fall within the range of approximately

30.58–38.0 dB. This fine-tuning strategy enables the model to adapt its encoding and decoding behavior to the realistic SNR dynamics of LEO satellite links, thereby improving reconstruction quality across the entire overpass, with particular emphasis on the high-SNR regimes encountered at moderate to high elevation angles.

As shown in Fig. 4, the fine-tuned model achieves significantly better reconstruction quality across the entire SNR range (1–38 dB) in terms of both PSNR and MS-SSIM compared to the base model when a moderate channel dimension ($C = 96$) is adopted. Moreover, when the SNR exceeds 5 dB, the fine-tuned model yields PSNR above 30.8 dB and MS-SSIM above 0.95.

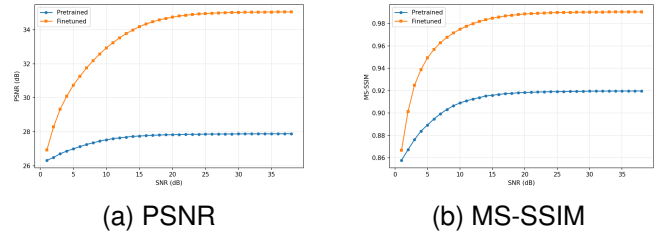


Fig. 4. Results of model finetuning.

2) *DRL Training*: During training, the RL agent operates in a simulated environment where the original images are readily available at the gateway. This allows immediate computation of PSNR and MS-SSIM after each transmission, providing instant reward signals for policy optimization.

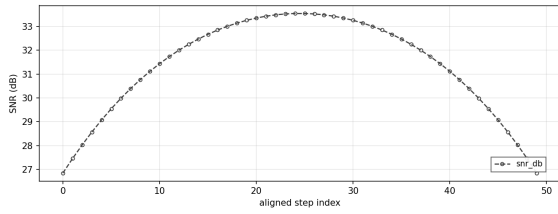
C. Simulation Results

1) *SNR sweep and rate adjust*: To emulate a full satellite overpass, the elevation angle θ is swept from 0° up to 90° and then back to 0° . The instantaneous SNR, obtained from the link budget calculation, exhibits a characteristic low–high–low trajectory over the visibility window, as shown in Fig. 5a. The evolution of the target rate under different policies is shown in Fig. 5b. The fixed-rate baselines, `min_rate`, `mid_rate`, and `max_rate`, adopt constant channel numbers $C = 32$, 96, and 192, respectively. In contrast, `rl_dqn` starts at 96.0, then after step 10 jumps to 128.0, and later returns to 96.0 at step 41, illustrating adaptive rate adjustment based on channel conditions and queue status. Figure 5c shows the transmission buffer occupancy of different policies during the entire SNR sweep. The `min_rate` and `mid_rate` policies maintain average occupancies of 6.7% and 20%, respectively. In contrast, `max_rate` saturates the buffer as early as step 5, leading to packet losses, with an average occupancy as high as 96.7%. For the proposed `rl_dqn` policy, the buffer occupancy stays at around 20% during the first 9 steps when the target rate is 96. From steps 10 to 40, the agent increases the target rate, causing the buffer utilization to rise steadily and peak at 91.2%. After the target rate decreases, the occupancy gradually drops to 62.5%. Notably, the proposed policy achieves high buffer utilization while incurring no packet loss throughout the entire process. Figure 5d and Table II present the per-step and overall performance of different policies. `max_rate` achieves

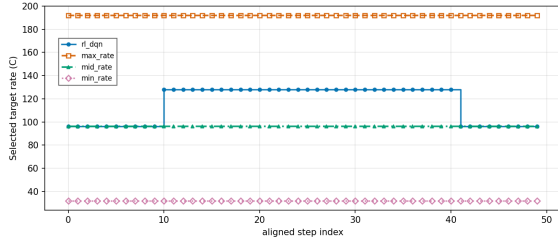
TABLE II
COMPARISON OF DIFFERENT POLICY ON TOTAL QUALIFIED FRAMES RECEIVED.

Policy	Qualified	Forwarded	Dropped	Mean Ch_num	Mean CBR	Qual/Fwd (%)
rl_dqn	524	564	0	115.84	0.076241	92.91
max_rate	343	343	228	192.00	0.12500	100.00
mid_rate	499	588	0	96.00	0.062500	84.86
min_rate	250	588	0	32.00	0.020833	42.52

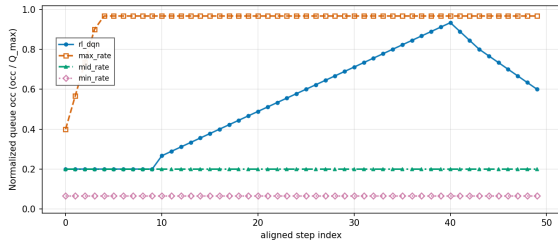
7 qualified frames per step but drops 228 frames in total due to buffer overflow, resulting in only 343 total qualified frames. `min_rate` avoids drops but only 42.52% of its forwarded frames are qualified (250 frames). Both `mid_rate` and `rl_dqn` have no drops, achieving qualified ratios of 84.86% and 92.91%, respectively. Notably, `rl_dqn` exploits favorable channel conditions by adopting a higher target rate, thereby obtaining more qualified frames than `mid_rate`.



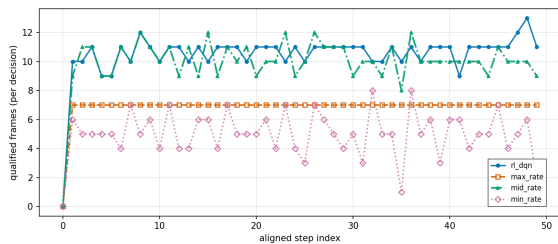
(a) SNR sweep



(b) Target rate adjust



(c) Tx_buffer occupancy



(d) Qualified Frames per step

Fig. 5. Process of SNR sweep and adjust of target rate at $\Gamma_{\text{PSNR}} = 32$ dB and $\Gamma_{\text{MS-SSIM}} = 0.94$.

2) *PSNR and MS-SSIM distributions of reconstructed images*: Figure 6 illustrates the distributions of PSNR and MS-SSIM for the reconstructed images, with the quality thresholds set to $\Gamma_{\text{PSNR}} = 32$ dB and $\Gamma_{\text{MS-SSIM}} = 0.94$, as indicated by the red dashed lines in the figure. From panels (a)–(d), it can be observed that, except for the `max_rate` policy, all other three strategies produce some PSNR values below the threshold, with `min_rate` having the most such instances. This result is consistent with expectations. Panels (e)–(h) show that, except for `min_rate`, the MS-SSIM values of the other three policies are consistently far above the threshold, typically around 0.99. Only `min_rate` occasionally drops to approximately 0.92. Therefore, unqualified frames are primarily caused by insufficient PSNR rather than MS-SSIM degradation.

3) *Visualization*: Figure 7 presents a side-by-side comparison of the original image and the reconstructed image with the *lowest* PSNR under each policy. The left column shows the original image, while the right column shows the reconstructed one. As expected, `min_rate` yields the poorest reconstruction quality (PSNR: 23.05 dB), `max_rate` achieves the best (PSNR: 32.29 dB), while both `mid_rate` and `rl_dqn` produce intermediate quality with PSNR values of 27.57 dB and 27.56 dB, respectively.

4) *Ablation Study: Impact of SNR Prediction*: To investigate the practical impact of SNR prediction, we train two policies — one with the SNR predictor module (`snr_pred_pl_only`) and one without (`wo_snr_pred`) — and compare their performance in terms of target rate adaptation and the final number of qualified frames. As shown in Fig. 8, the policy without SNR prediction selects the $C = 128$ level and keeps it unchanged, implying that no rate switching is performed over the entire SNR sweep. As a result, the transmission buffer becomes full at step 32, leading to a small number of dropped frames (17 frames). In contrast, the policy equipped with SNR prediction proactively adjusts the target rate based on the forecasted SNR, thereby avoiding buffer overflow and achieving a higher number of qualified frames. This confirms that SNR prediction enables timely rate adaptation, prevents congestion, and improves overall transmission efficiency.

5) *Ablation Study: Effect of SNR Prediction on Channel ModNet*: We compare two RL-based policies: one that feeds the predicted SNR to both the RL agent and the Channel ModNet, denoted as `snr_pred_encoder`, and the other that supplies the predicted SNR only to the RL agent (while the Channel ModNet uses the instantaneous SNR), denoted as `snr_pred_pl_only`. This isolates the impact of predictive channel information on the encoding adaptation process. As shown in Table III, no significant performance difference is observed between the two variants under the current smoothly

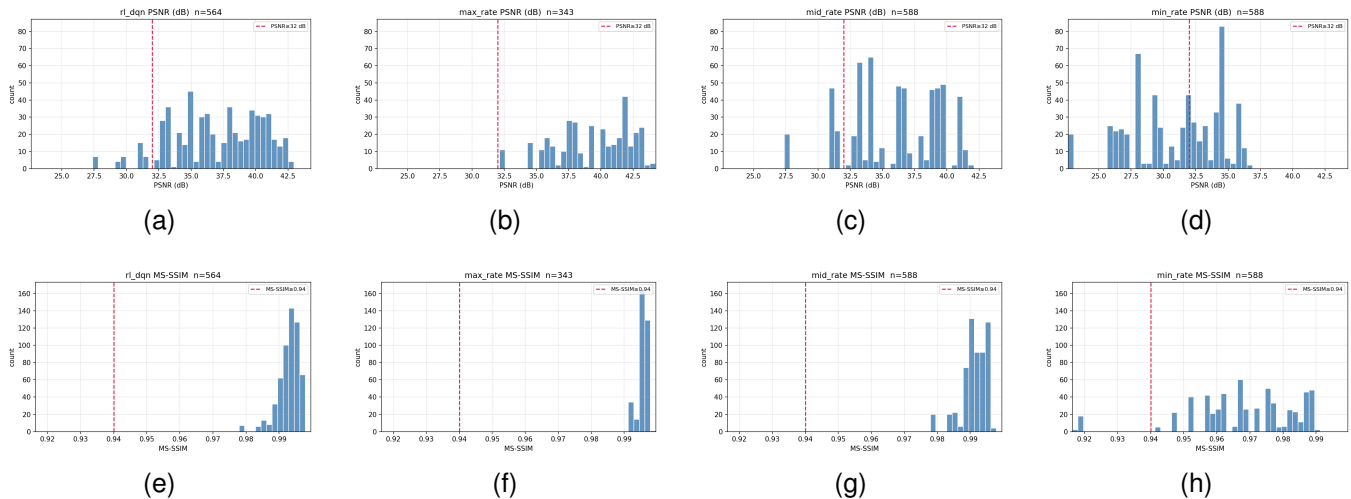


Fig. 6. Distributions of PSNR (a–d) and MS-SSIM (e–h) for reconstructed images. (a)–(d) show PSNR for `rl_dqn`, `max_rate`, `mid_rate`, and `min_rate`, respectively; (e)–(h) show the MS-SSIM distributions for the same four methods.

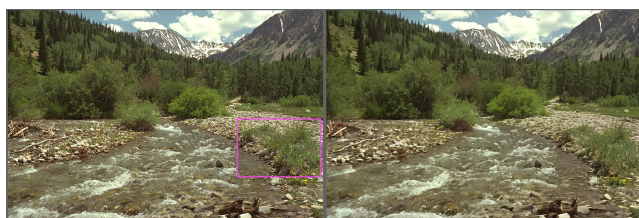
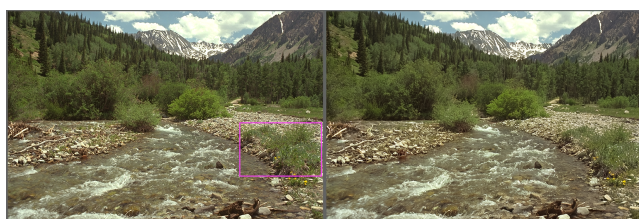


Fig. 7. Comparison of reconstruction quality for the lowest-PSNR image per policy. Left: original; right: reconstructed.

varying SNR scenario. The primary reason is that the SwinJSCC encoder and the Channel ModNet have already been fine-tuned to accommodate the entire SNR range of interest. In our experiments, the SNR trajectory generated by the link budget model changes very gradually over time, and the prediction horizon does not provide sufficient additional gain to meaningfully affect the reconstruction quality. Consequently, the benefit of feeding predicted SNR into the Channel ModNet is marginal in this setting, while its contribution to the RL agent’s rate decision remains essential for avoiding buffer overflow and improving throughput.

VI. CONCLUSIONS

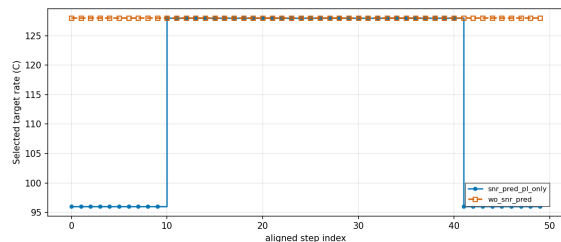
In this paper, we have proposed an adaptive semantic communication framework for LEO satellite-to-ground image transmission based on SwinJSCC. To address the dynamic nature of the satellite link and limited on-board resources, we introduced a transmission buffer and a link budget model to simulate SNR evolution over an overpass. A reinforcement learning agent dynamically selects the compression ratio at each decision interval, supported by a lightweight polynomial-based SNR predictor that compensates for control loop latency.

Simulation results demonstrate that the proposed RL-based policy significantly outperforms fixed-rate baselines in terms of qualified frame rate and buffer management, achieving no packet loss. SNR prediction proves vital for proactive rate adaptation, preventing overflow and improving throughput. The framework effectively balances transmission efficiency and reconstruction quality, offering a promising solution for real-time multi-spectral image downlink on resource-constrained LEO satellites.

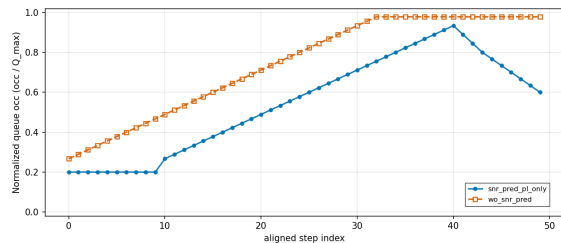
Future work includes extending the framework to multi-overpass scenarios, incorporating realistic channel impairments such as rain fading and scintillation, and exploring more advanced RL algorithms.

TABLE III
ABLATION STUDY ON THE IMPACT OF SNR PREDICTION.

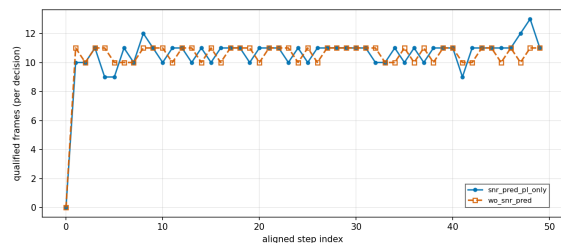
Metrics	wo_snr_pred	snr_pred_pl_only	snr_pred_encoder
qualified	521	524	524
forwarded	539	564	564
dropped	17	0	0
mean_channel_number	128.00	115.84	115.84
cbr_at_fwd	0.0833	0.0762	0.0762
qual/fwd (%)	96.660	92.908	92.908



(a) Target rate adjust



(b) Tx_buffer occupancy



(c) Qualified Frames per step

Fig. 8. Impact of SNR predict on performance of proposed RL policy.

REFERENCES

- [1] C. Sun, Y. Zhang, B. Tao, D. Vasisht, and M. Marina, “Deepspace: Super resolution powered efficient and reliable satellite image data acquisition,” in *Proceedings of the ACM SIGCOMM 2025 Conference*, ser. SIGCOMM ’25. New York, NY, USA: Association for Computing Machinery, 2025, p. 311–328. [Online]. Available: <https://doi.org/10.1145/3718958.3750523>
- [2] P. Zhang, W. Xu, H. Gao, K. Niu, X. Xu, X. Qin, C. Yuan, Z. Qin, H. Zhao, J. Wei, and F. Zhang, “Toward wisdom-evolutionary and primitive-concise 6g: A new paradigm of semantic communication networks,” *Engineering*, vol. 8, pp. 60–73, 2022. [Online]. Available: <https://www.engineering.org.cn/engi/EN/10.1016/j.eng.2021.11.003>
- [3] E. Bourtsoulatze, D. Burth Kurka, and D. Gündüz, “Deep joint source-channel coding for wireless image transmission,” *IEEE Transactions on Cognitive Communications and Networking*, vol. 5, no. 3, pp. 567–579, 2019.
- [4] K. Yang, S. Wang, J. Dai, X. Qin, K. Niu, and P. Zhang, “Swinjscc: Taming swin transformer for deep joint source-channel coding,” *IEEE Transactions on Cognitive Communications and Networking*, vol. 11, no. 1, pp. 90–104, 2025.
- [5] J. Xu, B. Ai, W. Chen, A. Yang, P. Sun, and M. Rodrigues, “Wireless image transmission using deep source channel coding with attention modules,” *IEEE Transactions on Circuits and Systems for Video Technology*, vol. 32, no. 4, pp. 2315–2328, 2022.
- [6] Y. Guo, C. Zhang, Y. Gong, and C. He, “Satellite transmission with joint source-channel coding under stochastic processes,” in *2024 16th International Conference on Wireless Communications and Signal Processing (WCSP)*, 2024, pp. 1031–1036.
- [7] Y. Jiang, K. Xie, Y. Ouyang, J. Wen, G. Zhang, W. Liang, and Q. Feng, “High quality compression and transmission of remote sensing images based on semantic communication,” *IEEE Transactions on Sustainable Computing*, vol. 10, no. 5, pp. 843–857, 2025.
- [8] Z. Tan, C. Liu, K. Xie, Y. Ouyang, J. Wen, G. Zhang, D. Chen, G. Xie, and K. Li, “Adaptive semantic communication system for high-quality remote sensing image transmission in unstable wireless environments,” *IEEE Transactions on Wireless Communications*, vol. 25, pp. 3001–3015, 2026.
- [9] Z. Li and Q. Yang, “Channel-adaptive semantic satellite communication for remote sensing images,” in *ICC 2025 - IEEE International Conference on Communications*, 2025, pp. 6910–6915.
- [10] Y. Yin, S. Liu, D. Wen, Y. Wu, and Y. Shi, “Joint source and channel coding for multi-modal satellite-to-ground semantic communications,” in *2025 IEEE Wireless Communications and Networking Conference (WCNC)*, 2025, pp. 01–06.
- [11] W. Zhang, H. Zhang, H. Ma, H. Shao, N. Wang, and V. C. M. Leung, “Predictive and adaptive deep coding for wireless image transmission in semantic communication,” *IEEE Transactions on Wireless Communications*, vol. 22, no. 8, pp. 5486–5501, 2023.